Synthesis and Characterization of Some Heterometal-Substituted Ammonium Gallophosphates

Arian R. Overweg,*,† Jan W. de Haan,† Pieter C. M. M. Magusin,† Rutger A. van Santen,† Gopinathan Sankar,‡ and John Meurig Thomas‡

Schuit Institute of Catalysis, Laboratory of Inorganic Chemistry and Catalysis, Eindhoven University of Technology, P.O.Box 513, 5600 MB Eindhoven, The Netherlands, and Davy Faraday Research Laboratory, The Royal Institution of Great Britain, 21 Albemarle Street, London, W1X 4BS, United Kingdom

Received September 14, 1998. Revised Manuscript Received March 1, 1999

Various metal-substituted ammonium gallophosphates (metal is Zn, Mn, Mg, and Fe) have been synthesized. Characterization by X-ray diffraction (XRD), X-ray absorption spectroscopy (XAS), and ^{31}P MAS and ^{71}Ga MAS NMR shows that the structures are similar and isostructural to the known ammonium cobalt gallophosphate hydrate, $[NH_4][CoGa_2P_3O_{12}\text{-}(H_2O)_2]$. It is concluded from a combined in situ XRD/XAS study that the gallophosphate molecular sieves described here are not thermally stable and lose their microporous nature above 350 °C.

Introduction

The promising potential applications of crystalline, microporous materials as ion-exchange materials,[1] molecular sieves,[2] and catalysts[3] has led to a lively quest for open framework structures. The discovery of the family of alumino phosphate (ALPO) molecular sieves by Wilson in 1982[4] was an important step forward and uncovered a whole new area of materials with an amazing structural variety, ranging from very small pore ALPOs, such as ALPO-4 with pores of ∼3 Å to the large pore VPI-5, with pore diameters of ∼12 Å.

In contrast to zeolites a large variety of heteroatoms can easily be incorporated in the ALPO structure by substitution of Al and/or P. Consequently, this leads to a modification of the physical and chemical properties of the parent material. In particular, the substitution by lower valent metal ions, illustrated by the substitution of trivalent Al by divalent transition metal ions or partial replacement of pentavalent P by tetravalent Si, is highly interesting since it gives rise to a negatively charged framework which is compensated by cations. In this way it proved possible to introduce Brønsted acidity and make these microporous materials potential solid-acid catalysts. Some of these materials indeed show an enhanced catalytic activity. In this respect the conversion of methanol to light olefins by several substituted ALPOs has received considerable attention.[5−7] Additionally, the incorporation of divalent transition metals (e.g., Ti, V, Cr, Mn, or Co) into the lattice also produces good redox molecular sieve catalysts.[8]

Parallel to the discovery of many novel ALPO structures, a number of gallophosphates with an open framework structure were brought to light. Some of these structures are similar to the corresponding ALPO molecular sieves[9−17] but also new, unique structures were found.[18−29] Recently, the synthesis and structural

* Corresponding author.
† Schuit Institute of Catalysis.
‡ Davy Faraday Research Laboratory.

(1) Townsend, R. P. *Introduction to Zeolite Science and Practice*; van Bekkum, H., Flanigen, E. M., Jansen, J. C., Eds.; Studies in Surface Science and Catalysis; Elsevier: Amsterdam, 1991; Vol. 58, p 359.
(2) Flanigen, E. M. *Proc. Intl. Conf. Zeolites* Rees, L.V. C., Ed.; Naples, Italy, **1980**, *5*, 760.
(3) Thomas, J. M. *Angew. Chem., Int. Ed. Engl.* **1988**, *27*, 1673.
(4) Wilson, S. T.; Lok, B. M.; Messing, C. A.; Cannan, T. R.; Flanigen, E. M. *J. Am. Chem. Soc.* **1982**, *104*, 1146.
(5) Chen, J.; Dakka, J.; Neelman, E.; Sheldon, R. A. *J. Chem. Soc., Chem. Commun.* **1993**, 1379.
(6) Chen, J.; Thomas, J. M. *J. Chem. Soc., Chem. Commun.* **1994**, 603.
(7) Smith, L.; Cheetham, A, K.; Marchese, L.; Thomas, J. M.; Wright, P. A.; Chen, J.; Gianotti, E. *Catal. Lett.* **1996**, *41*, 13.
(8) Sheldon, R. A.; Dakka, J., *Catal. Today* **1994**, *19*, 215.
(9) Chen, J.; Sankar, G.; Thomas, J. M.; Xu, R.; Greaves, G. N.; Waller, D. *Chem. Mater.* **1992**, *4*, 1373.
(10) Parise, J. B. *J. Chem. Soc., Chem. Commun.* **1985**, 606.
(11) Parise, J. B. *Inorg. Chem.* **1985**, *24*, 4312.
(12) Parise, J. B. *Acta Crystallogr., Sect. C* **1986**, *42*, 670.
(13) Parise, J. B. *Acta Crystallogr., Sect. C* **1986**, *42*, 144.
(14) Simmen, A.; Patarin, J.; Baerlocher, Ch. *Proc. Int. Zeol. Conf.* Montreal, **1993**, *9*, 433.L
(15) Loiseau, T.; Riou, D.; Licheron, M.; Ferey, G. *J. Solid State Chem.* **1994**, *111*, 397.
(16) Loiseau, T.; Ferey. G. *Eur. J. Solid State Inorg. Chem.* **1994**, *31*, 575.
(17) Yang, G.; Feng, S.; Xu, R *J. Chem. Soc., Chem. Commun.* **1987**, 1254.
(18) Wang, T.; Yang, G.; Feng, S.; Shang, C.; Xu, R. *J. Chem. Soc., Chem. Commun.* **1989**, 948.
(19) Jones, R. H.; Thomas, J. M.; Huo, Q.; Xu, R.; Hursthouse, M. B.; Chen, J. *J. Chem. Soc., Chem. Commun.* **1991**, 1520.
(20) Estermann, M.; McCusker, L. B.; Baerlocher, Ch.; Merrouche, A.; Kessler, H. *Nature* **1991**, 320.
(21) Loiseau, T.; Férey, G. *J. Chem. Soc., Chem. Commun.* **1992**, 1197.
(22) Kan, Q.; Glasser, F. P.; Xu, R. *J. Mater. Chem.* **1993**, *3*, 983.
(23) Yin, X.; Nazar, L. F. *J. Chem. Soc., Chem. Commun.* **1994**, 2349.
(24) Loiseau, T.; Riou, D.; Taulelle, F.; Férey, G. *Stud. Surf. Sci. Catal.* **1994**, *84*, 395.
(25) Feng, S.; Xu, X.; Yang, G.; Xu, R.; Glasser, F. P. *J. Chem. Soc., Dalton Trans.* **1995**, 2147.
(26) Attfield, M. P.; Morris, R. E.; Gutierrez-Puebla, E.; Monge-Bravo, A.; Cheetham, A. K. *J. Chem. Soc., Chem. Commun.* **1995**, 843.
(27) Chippindale, A. M.; Walton, R. I.; Turner, C. *J. Chem. Soc., Chem. Commun.* **1995**, 1261.
(28) Lii, K.-H. *Inorg. Chem.* **1996**, *35*, 7440.

10.1021/cm9806331 CCC: $18.00
Published on Web 06/30/1999

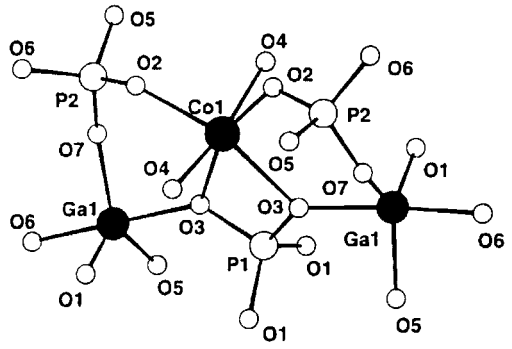

Figure 1. Local structure of ammonium cobalt gallophosphate (reproduced by permission of the Royal Society of Chemistry).

characterization of a number of heterometal-substituted gallophosphates has also been reported.[30−35] In the majority of cases,[30,31,33,35] the heterometal substitutes for Ga atoms in the framework and forms tetrahedra together with O atoms but two microporous gallophosphate materials, $[NH_4][CoGa_2P_3O_{12}(H_2O)_2]$[32] and $[C_6N_2H_{14}][MnGa(PO_3OH)(PO_4)]$,[34] have been found with unique framework positions of the heterometal. In these structures the heterometal has a coordination state different from the other elements in the material.

Here, we present the incorporation of the divalent ions of Zn, Mn, Mg, and Fe into gallophosphate open framework structures which are similar to the ammonium cobalt gallium phosphate hydrate, $[NH_4][CoGa_2P_3O_{12}(H_2O)_2]$.[32] The structure of this material is built up of GaO_5, CoO_6, and PO_4 units, as depicted in Figure 1. The GaO_5 building units occur as distorted trigonal bipyramids, while the CoO_6 units have a distorted octahedral symmetry. The two O(4) oxygen atoms connected to the Co atom are assigned to bonded water molecules. The negative charge of the framework is balanced by ammonium ions which are located in parallel, nearly circular channels with dimensions ~6.0 Å × 7.4 Å. These channels are intersected by a collection of smaller channels with a more or less elliptical shape and shortest cross-channel O···O distances of ~4.0 Å × 4.3 Å, thus forming a three-dimensional network of pores. In this study we focus on the synthesis and characterization of these compounds using powder X-ray diffraction (XRD), X-ray absorption spectroscopy (XAS), solid-state ^{31}P and ^{71}Ga NMR, and Mössbauer spectroscopy. Because of their potential as solid acids we also studied the thermal stability of these materials in air by recording both XRD patterns and XAS spectra in a combined experiment as a function of temperature. Although the present study enabled us to gather more insight into these novel materials, the combined in situ XRD/XAS technique showed that these materials are not thermally stable and lose their microporous structure above 350 °C.

Table 1. Gel Composition

$1Ga_2O_3:5(NH_4)_2HPO_4:10H_3PO_4:156H_2O:0.3Si(OCH_2CH_3)_4:1Me$

[a] Me = metal source, CoO, $Zn(OOCCH_3)_2\cdot 2H_2O$, $Mn(OOCCH_3)_2\cdot 4H_2O$, and $Mg(OOCCH_3)_2\cdot 4H_2O$, $Fe(OOCCH_3)_2$, respectively.

Experimental Section

Synthesis. The five title compounds were crystallized from a gel composition containing Ga_2O_3 (Aldrich, 99.99%), H_3PO_4 (Aldrich, 85% by mass), $(NH_4)_2HPO_4$ (Aldrich, 99%), $Si(OCH_2CH_3)_4$ (Aldrich, 98%), H_2O, and a metal source, CoO (Aldrich), $Zn(OOCCH_3)_2\cdot 2H_2O$ (Aldrich, 98+%), $Mn(OOCCH_3)_2\cdot 4H_2O$ (Aldrich, 99+%), $Mg(OOCCH_3)_2\cdot 4H_2O$, and $Fe(OOCCH_3)_2$ (Aldrich, 95%), respectively, as shown in Table 1. Typically, 0.5 g of Ga_2O_3 and a proper amount of the metal source were mixed together with 7.5 mL of water and a few drops of $Si(OCH_2CH_3)_4$, which acts as a mineralizing agent. $(NH_4)_2HPO_4$ was then added, and the mixture was stirred for 10 min followed by the addition of phosphoric acid and additional stirring until the gel was of a uniform composition. Subsequently, the gel was transferred into a Teflon-lined stainless steel autoclave and heated at 190 °C for 6 days. After cooling, the solid material was collected by filtration, washed with demineralized water, and dried at 343 K overnight. A purer phase was obtained in a second synthesis if, instead of $Si(OCH_2CH_3)_4$, a small amount of the appropriate gallophosphate was used as the seed.

Characterization. X-ray diffraction data were collected on a Siemens D500 diffractometer using Cu Kα radiation. Elemental analyses were performed by atomic absorption spectroscopy (Me, Ga) using a Perkin-Elmer 3030 atomic absorption spectrophotometer and by photometry (P) using a Hitachi 150−20 Spectrophotometer. To determine the weight loss as a function of temperature thermographic analyses were carried out in air using a Shimadzu TGA-50 thermographic analyzer. The samples were heated in air to 650 °C at a rate of 5 °C/min. Mössbauer spectra were recorded at 293 K with a constant acceleration spectrometer. The isomer shift was recorded relative to sodium nitroprusside (snp).

Magic angle spinning ^{31}P NMR experiments were performed on a Bruker MSL 400 at 9.4 T equipped with a Standard Bruker 4-mm MAS probehead. Sample spinning speeds of 8 kHz were applied, and chemical shifts are reported relative to 85 wt % H_3PO_4. A single-pulse excitation program was used with a 90° pulse of 3.8 μs and a repetition delay of 60 s. Constant overall time (COT) ^{31}P NMR spectra were obtained at a MAS rate of 10 kHz and an overall time of 12.8 ms using the method basically described elsewhere.[36] A series of 64 Hahn echoes with varied echo times were recorded with a time resolution of 200 μs in both the echo-time and real-time dimension. From the resulting two-dimensional signal $S(t_1,t_2)$, the data points with $t_1 + t_2 = 12.8$ ms were collected. These data points were used to replace the first 64 data points in the echo recorded for $t_1 = 200$ μs. Fourier transformation of the resulting signal yields a COT spectrum in which the homogeneous broadening is largely removed at the cost of an intensity reduction. Magic angle spinning ^{71}Ga NMR spectra were recorded on a Chemagnetics CMX 400 at 9.4 T. Spinning speeds of ~23 kHz were necessary to obtain well-resolved spectra using a Chemagnetics 3.2-mm BB-H probehead. A pulse length of 1 μs was chosen corresponding to a flip angle of ~25° with a repetition time of 1s. The resonances were recorded relative to a 1.0 M $Ga(NO_3)_3$ solution. Simulations of the ^{31}P MAS and ^{71}Ga MAS NMR experiments were carried out with the WINFIT software (Bruker, Rheinstetten, Germany).

The XAS measurements of the Co K-edge, the Zn K-edge, and the Ga K-edge of the as-prepared samples were carried out on station 7.1 of the CLRC, Daresbury Synchrotron Radiation Source. This station is equipped with a Si(111) monochromator and ion chambers in order to obtain data in

(29) Weigel, S. J.; Weston, S. C.; Cheetham, A. K.; Stucky, G. D. *Chem. Mater.* **1997**, *9*, 1293.
(30) Chippindale, A. M.; Walton, R. I. *J. Chem. Soc., Chem. Commun.* **1994**, 2453.
(31) Cowley, A. R.; Chippindale, A. M. *Chem. Commun.* **1996**, 673.
(32) Chippindale, A. M.; Cowley, A. R.; Walton, R. I. *J. Mater. Chem.* **1996**, *6*, 611.
(33) Chippindale, A. M.; Cowley, A. R. *Zeolites* **1997**, *18*, 176.
(34) Chippindale, A. M.; Bond, A. D.; Cowley, A. R.; Powell, A. V. *Chem. Mater.* **1997**, *9*, 2830.
(35) Bond, A.D.; Chippindale, A. M.; Cowley, A. R.; Readman, J. E.; Powell, A. V. *Zeolites* **1997**, *19*, 326.
(36) Magusin, P. C. M. M.; Veeman, W. S. *J. Magn. Reson. Ser. A* **1996**, *119*, 252.

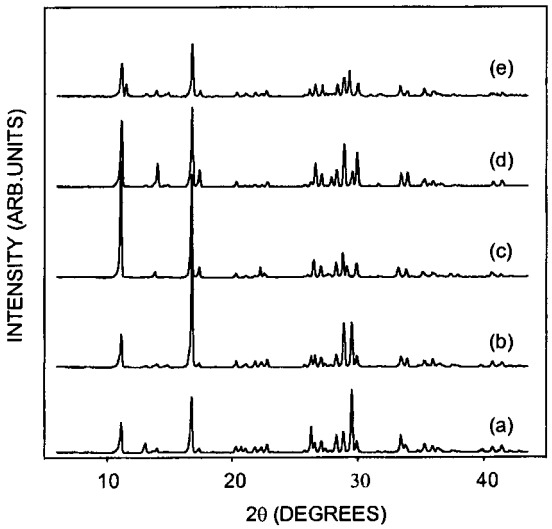

Figure 2. X-ray powder diffraction patterns of (a) $NH_4[CoGa_2P_3O_{12}(H_2O)_2]$, (b) $NH_4[ZnGa_2P_3O_{12}(H_2O)_2]$, (c) $NH_4[MnGa_2P_3O_{12}(H_2O)_2]$, (d) $NH_4[MgGa_2P_3O_{12}(H_2O)_2]$, and (e) $NH_4[FeGa_2P_3O_{12}(H_2O)_2]$.

the transmission mode. Station 9.3 of the CLRC, Daresbury Synchrotron Radiation Source was used to perform combined XAS-XRD measurements.[37] This station is equipped with a Si(220) monochromator, ion chambers, and a curved position-sensitive detector. Self-supporting wafers of the samples were mounted on a specially designed cell and the sample was heated in air at a heating rate of 5 °C/min to 625 °C and held at this temperature for 1 h. After this, the sample was allowed to cool to room temperature. During the course of heating the sample, data were recorded sequentially with XRD measurements being conducted for 180 s, and XAS was measured for 380 s, giving rise to a total time of 10 min, which includes the dead time of 40 s. All the XRD measurements were carried out ~100 eV below the metal K-edge adsorption to avoid fluorescence effects, and the wavelengths are given in the respective figure captions. The data were analyzed using the set of programs available at the Daresbury Laboratory, UK. EXCALIB and EXBROOK were used for calibration and background subtraction, data fitting was carried by use of EXCURV92.[38] $[NH_4][CoGa_2P_3O_{12}(H_2O)_2]$, $ZnAl_2O_4$, and MnO_2, all with known octahedral (Co, Zn, Mn) or trigonal bipyramidal (Ga) coordination, were used as model compounds so as to yield the nonstructural parameter associated with EXAFS.

Results and Discussion

The X-ray diffraction patterns of the five heterometal-substituted ammonium gallophosphates are presented in Figure 2. All reflections in the patterns could readily be indexed on the basis of the monoclinic unit cell with space group *C*2/*c* as was established earlier by ref 32. The gallophosphate containing iron however showed a few extra reflections due to the presence of a crystalline contamination. This was confirmed by Mössbauer spectroscopy revealing an Fe(III) impurity (see Figure 3). The isomer shift and quadrupole splitting of the phase corresponding to the ammonium iron gallophosphate, $NH_4[FeGa_2P_3O_{12}(H_2O)_2]$, is in good agreement with values found for $Fe^{II}PO_4$ compounds.[39] From chemical

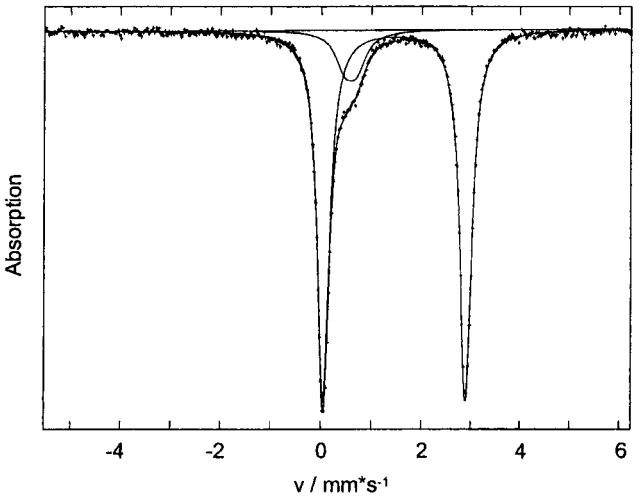

Figure 3. Mössbauer spectrum of $NH_4[FeGa_2P_3O_{12}(H_2O)_2]$. The signal with isomer shift (IS), 1.499 mm s^{-1}, and quadrupole splitting (QS), 2.852 mm s^{-1} was assigned to the ammonium iron gallophosphate hydrate. The signal with parameters, IS, 0.606 mm s^{-1} and small QS, 0.236 mm s^{-1}, was assigned to an Fe(III) impurity.

Table 2. Elemental Analysis (Calculated Values in Parentheses)

sample	C (%)	H (%)	N (%)
$NH_4[CoGa_2P_3O_{12}(H_2O)_2]$	0.03 (0)	1.49 (1.50)	2.63 (2.61)
$NH_4[ZnGa_2P_3O_{12}(H_2O)_2]$	0.03 (0)	1.51 (1.48)	2.51 (2.58)
$NH_4[MnGa_2P_3O_{12}(H_2O)_2]$	0.02 (0)	1.58 (1.51)	2.62 (2.63)
$NH_4[MgGa_2P_3O_{12}(H_2O)_2]$	0.04 (0)	1.62 (1.60)	2.75 (2.79)
$NH_4[FeGa_2P_3O_{12}(H_2O)_2]$	0.03 (0)	1.60 (1.51)	2.68 (2.62)

analyses a Me:Ga:P ratio of 1:2:3 was found for all samples and the presence of H_2O and NH_4 ions was confirmed by C,H,N analyses (see Table 2). Thermographic analysis showed that all materials lose weight gradually over the temperature range 250−600 °C. A larger weight loss was obtained than could be accounted for on the basis of loss of water and ammonia molecules only. As will be discussed later combined XRD/XAS showed that the materials lose their structural integrity upon heat treatment. Therefore, it can be argued that volatile decomposition products probably are responsible for this larger weight loss.

^{31}P MAS NMR spectra of the diamagnetic gallophosphates, $NH_4[ZnGa_2P_3O_{12}(H_2O)_2]$ and $NH_4[MgGa_2P_3O_{12}(H_2O)_2]$ are presented in Figure 4. Both spectra show two signals in a ratio of approximately 2:1. This confirms the assumption based on the powder X-ray diffraction patterns that the framework structures of these materials are similar to that of the ammonium cobalt gallophosphate hydrate, $NH_4[CoGa_2P_3O_{12}(H_2O)_2]$. In this compound two crystallographically different P atoms are present in a ratio of 2:1.[32] The zinc gallophosphate has peaks located at −10.7 and −11.8 ppm while chemical shift values at −12.2 and −12.8 ppm were obtained for the magnesium-containing material. These values agree well with chemical shift range found for other gallophosphates reported in the literature.[24,40,41]

The ^{31}P COT spectrum of $NH_4[MgGa_2P_3O_{12}(H_2O)_2]$ presented in Figure 5 shows a considerable improve-

(37) Sankar, G.; Wright, P. A.; Natarajan, S.; Thomas, J. M.; Greaves, G. N.; Dent, A. J.; Dobson, B. R.; Ramsdale, C. A.; Jones, R. H. *J. Phys. Chem.* **1993**, *97*, 9550.

(38) Binsted, N.; Campbell, J. W.; Gurman, S. J.; Stephenson, P. C. CCLRC Daresbury Laboratory EXCURV92 program, 1991.

(39) Berry, F. J.; Maddock, A. G. *J. Chem. Soc., Chem. Commun.* **1978**, 308.

(40) Merrouche, A.; Patarin, J.; Kessler, H.; Soulard, M.; Delmotte, L.; Guth, J. L. *Zeolites* **1992**, *12*, 226.

(41) Bradley, S. M.; Howe, R. S.; Hanna, J. V. *Solid-State Nucl. Magn. Reson.* **1993**, *2*, 37.

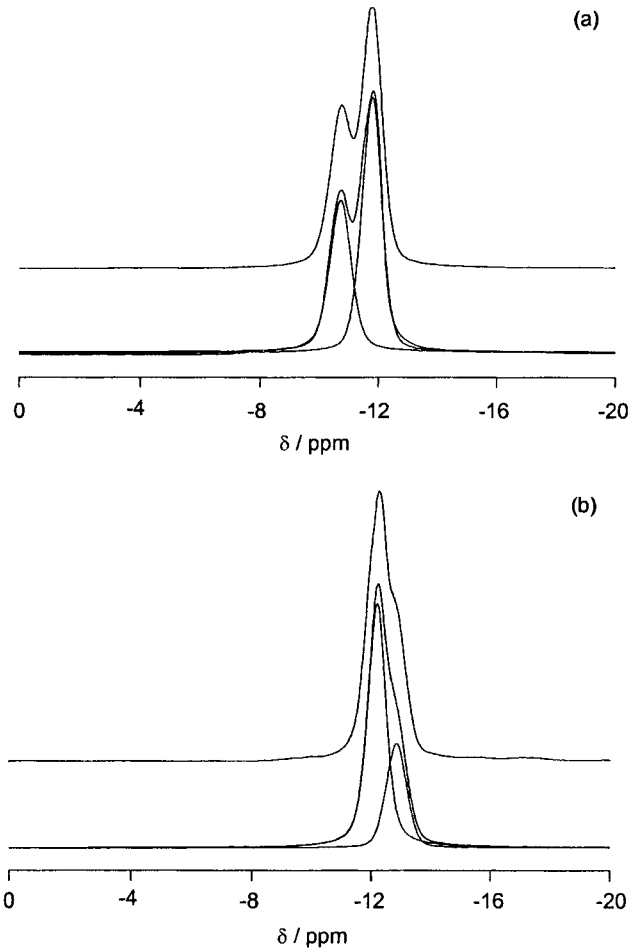

Figure 4. Experimental and simulated ^{31}P MAS NMR spectra of (a) $NH_4[ZnGa_2P_3O_{12}(H_2O)_2]$ and (b) $NH_4[MgGa_2P_3O_{12}(H_2O)_2]$.

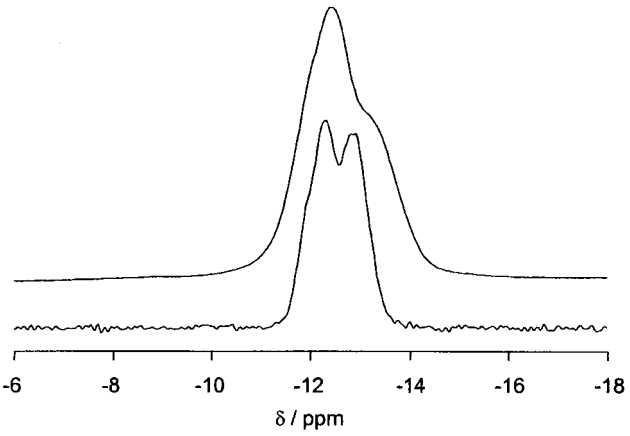

Figure 5. ^{31}P MAS NMR spectra of $NH_4[MgGa_2P_3O_{12}(H_2O)_2]$ (a) with and (b) without homogeneous line broadening.

ment of the spectral resolution, indicating that the nature of the line broadening observed in the ^{31}P MAS NMR spectrum of this material is largely homogeneous. Despite suppressing homogeneous line broadening by magic angle spinning some residual homogeneous line broadening always remains. This can severely hamper the interpretation of spectra where the line positions are in close proximity as, for example, is observed in a number of zeolite and ALPO molecular sieves. The observation here that a large part of the line broadening in the ^{31}P MAS NMR spectrum is caused by homogeneous effects might be of importance to the assignment

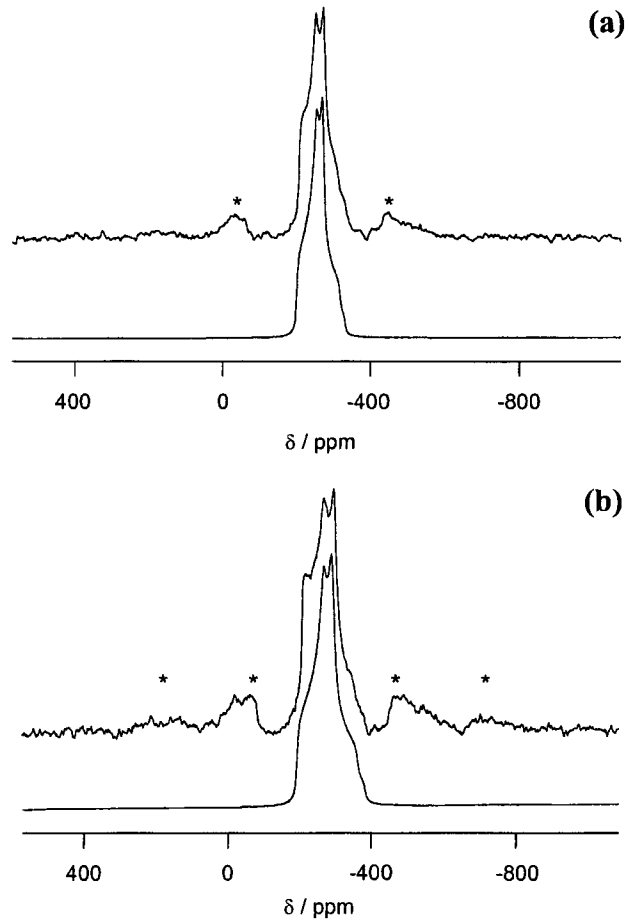

Figure 6. ^{71}Ga MAS NMR spectra of (a) $NH_4[ZnGa_2P_3O_{12}(H_2O)_2]$ and (b) $NH_4[MgGa_2P_3O_{12}(H_2O)_2]$.

Table 3. Chemical Shifts and Quadrupole Interaction Parameters for ^{71}Ga in $NH_4[ZnGa_2P_3O_{12}(H_2O)_2]$ and $NH_4[MgGa_2P_3O_{12}(H_2O)_2]$[a]

material	δ_{iso} (ppm)	QCC (MHz)	η
$NH_4[ZnGa_2P_3O_{12}(H_2O)_2]$	49.0	5.44	0.66
$NH_4[MgGa_2P_3O_{12}(H_2O)_2]$	55.9	6.36	0.60

[a] Abbreviations: δ_{iso}, isotropic chemical shift; QCC, quadrupole coupling constant; η, asymmetry parameter

of NMR lines to crystallographic positions in other molecular sieves.

Figure 6 shows the experimental ^{71}Ga MAS NMR spectra of $NH_4[ZnGa_2P_3O_{12}(H_2O)_2]$ (Figure 6a) and $NH_4[MgGa_2P_3O_{12}(H_2O)_2]$ (Figure 6b) together with the simulations. The NMR line-shape parameters are outlined in Table 3. The respective spectra reveal a single resonance at 49.0 and 55.9 ppm. This is in line with the crystallographic data which predict one crystallographic position for the Ga atoms. To the best of our knowledge these are the first examples of well-resolved ^{71}Ga NMR spectra of materials having only 5-fold coordinate Ga. ^{71}Ga NMR data of cloverite, where Ga also occupies a 5-fold coordinated position, have been reported in the literature,[40,41] but due to low spectral resolutions, no quadrupole parameters have been derived from these spectra. Considering this lack of reliable data in the literature a correlation between the NMR parameters obtained in this study and structural parameters cannot be given. A comparison between ^{27}Al NMR data and ^{71}Ga NMR data, however, predicts a

Table 4. Structural Parameters of the First and Second Coordination Shells around the Ga Atoms in As-Prepared Metal Gallophosphates As Obtained from Curve-Fitting Analysis of the Ga K-Edge EXAFS Data[a]

shell	atom	CN	d (Å)	σ^2 (Å^2)	shell	atom	CN	d (Å)	σ^2 (Å^2)	Ga−O−P angle (deg)
					$NH_4[CoGa_2P_3O_{12}(H_2O)_2]$					
1	O	1	1.99 (2.01)	0.0030	6	P	1	3.35 (3.26)	0.0052	134.5 (132.3)
2	O	1	1.86 (1.86)	0.0030	7	P	1	3.16 (3.10)	0.0052	132.3 (131.2)
3	O	1	1.87 (1.86)	0.0030	8	P	1	3.17 (3.15)	0.0052	137.3 (137.3)
4	O	1	1.92 (1.96)	0.0030	9	P	1	3.16 (3.14)	0.0052	128.7 (127.0)
5	O	1	1.77 (1.84)	0.0030	10	P	1	3.13 (3.17)	0.0052	140.7 (139.6)
					$NH_4[ZnGa_2P_3O_{12}(H_2O)_2]$					
1	O	1	2.01	0.0020	6	P	1	3.35	0.0044	134.0
2	O	1	1.88	0.0020	7	P	1	3.17	0.0044	131.8
3	O	1	1.84	0.0020	8	P	1	3.17	0.0044	137.9
4	O	1	1.94	0.0020	9	P	1	3.17	0.0044	128.3
5	O	1	1.82	0.0020	10	P	1	3.16	0.0044	140.0
					$NH_4[MnGa_2P_3O_{12}(H_2O)_2]$					
1	O	1	2.01	0.0038	6	P	1	3.19	0.0051	131.2
2	O	1	1.88	0.0038	7	P	1	3.19	0.0051	132.2
3	O	1	1.88	0.0038	8	P	1	3.23	0.0051	138.0
4	O	1	1.93	0.0038	9	P	1	3.19	0.0051	128.7
5	O	1	1.81	0.0038	10	P	1	3.31	0.0051	142.1
					$NH_4[MgGa_2P_3O_{12}(H_2O)_2]$					
1	O	1	2.02	0.0061	6	P	1	3.34	0.0060	133.4
2	O	1	1.89	0.0061	7	P	1	3.18	0.0060	131.6
3	O	1	1.87	0.0061	8	P	1	3.15	0.0060	137.0
4	O	1	1.91	0.0061	9	P	1	3.18	0.0060	129.0
5	O	1	1.82	0.0061	10	P	1	3.13	0.0060	139.6

[a] The numbers in parentheses are taken from crystallographic data as given by ref 32.

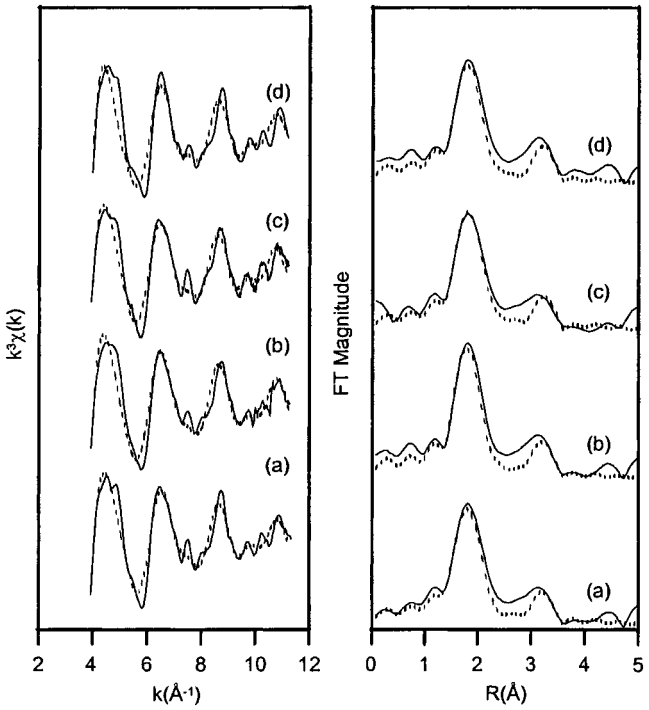

Figure 7. Ga K-edge EXAFS (on the left) and related FTs (on the right) of the as-prepared (a) $NH_4[CoGa_2P_3O_{12}(H_2O)_2]$, (b) $NH_4[ZnGa_2P_3O_{12}(H_2O)_2]$, (c) $NH_4[MnGa_2P_3O_{12}(H_2O)_2]$, and (d) $NH_4[MgGa_2P_3O_{12}(H_2O)_2]$. The solid lines represent the experimental data and the dotted lines show the calculated fits.

range for isotropic chemical shifts of pentacoordinated gallium atoms in gallophosphate materials of 40−70 ppm.[42] As can be seen from Table 3, the ^{71}Ga resonances observed here fit well within this range.

The local structure around Ga, Co, Zn, and Mn in the as-prepared samples has been probed by X-ray absorption spectroscopy. The Ga K-edge EXAFS spectra together with the corresponding Fourier transforms and the best fits are presented in Figure 7. The results of these fits are summarized in Table 4. The model used to fit the data is based on structural data from $NH_4[CoGa_2P_3O_{12}(H_2O)_2]$. The structure of this microporous gallophosphate, as determined by single-crystal XRD,[32] shows that the immediate environment of Ga is given by five O atoms with which it forms a distorted trigonal bipyramid. The Ga−O bond distances are distributed, ranging from 1.84 to 2.01 Å. In addition, the distances of the five P atoms in the second coordination sphere to the central Ga atom vary from 3.10 to 3.26 Å (see also Table 4, the numbers in parentheses are taken from the crystallographic data). At distances greater than 3.5 Å apart from the Ga atom a large number of oxygens atoms are found. Therefore, we adopted a simplified model to analyze the Ga environment by neglecting these remote atoms and taking into account only the nearest five O and P atoms. The model consists of five O and five P shells and multiple scattering was implemented in the calculation so as to obtain Ga−O−P bond angles. The Debye−Waller factors for the O shells and P shells, respectively, were constrained to be the same value. No refinement of the coordination numbers was carried out.

As can be seen from Table 4 the bond distances and bond angles of $NH_4[CoGa_2P_3O_{12}(H_2O)_2]$ as predicted by refinement of the EXAFS data are in good agreement with the crystallographic data reported earlier by ref 32. Therefore, we feel that on applying this model to refine the Ga K-edge data taken from the series of metal-substituted gallophosphates we obtain reliable structural parameters. Substitution of Co by Zn, Mn, or Mg causes only small changes in the local environment of the Ga atoms (see Table 4). The average Ga−O distance, which is a clear indication for the coordination state of the Ga atom, is 1.88 Å in the Co-substituted

(42) Bradley, S. M.; Howe, R. S.; Kydd, R. A. *Magn. Reson. Chem.* **1993**, *31*, 883.

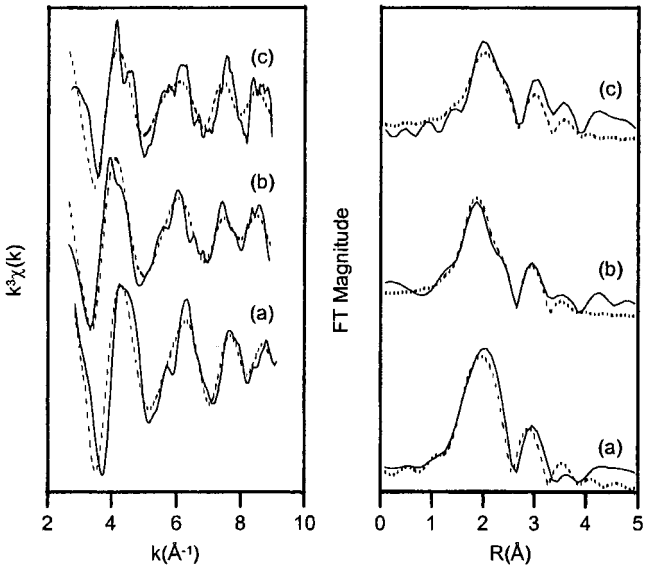

Figure 8. Me K-edge EXAFS (on the left) and the associated FTs (on the right) of as-prepared (a) $NH_4[CoGa_2P_3O_{12}(H_2O)_2]$, (b) $NH_4[ZnGa_2P_3O_{12}(H_2O)_2]$, and (c) $NH_4[MnGa_2P_3O_{12}(H_2O)_2]$ with Me is Co, Zn, and Mn, respectively. The experimental data are represented by solid lines, the dotted lines reflect the calculated fits.

Table 5. EXAFS Data Analysis of the First and Second Coordination Shells around the Me Atoms in the As-Prepared Metal Gallophosphates, $NH_4[CoGa_2P_3O_{12}(H_2O)_2]$, $NH_4[ZnGa_2P_3O_{12}(H_2O)_2]$, and $NH_4[MnGa_2P_3O_{12}(H_2O)_2]$[a]

shell	atom	CN	*d* (Å)	σ^2 (Å^2)	Co−O−P angle (deg)
		$NH_4[CoGa_2P_3O_{12}(H_2O)_2]$			
1	O	2	1.97 (2.01)	0.0105	
2	O	2	2.07 (2.15)	0.0105	
3	O	2	2.18 (2.19)	0.0105	
4	P	1	2.83 (2.82)	0.0088	99.2 (96.9)
5	P	2	3.21 (3.20)	0.0088	128.1 (130.7)
		$NH_4[ZnGa_2P_3O_{12}(H_2O)_2]$			
1	O	2	1.96	0.0131	
2	O	2	2.06	0.0131	
3	O	2	2.20	0.0131	
4	P	1	2.86	0.0122	101.1
5	P	2	3.23	0.0122	130.7
		$NH_4[MnGa_2P_3O_{12}(H_2O)_2]$			
1	O	2	2.11	0.0341	
2	O	2	2.14	0.0341	
3	O	2	2.26	0.0341	
4	P	1	2.94	0.0139	101.5
5	P	2	3.29	0.0139	127.7

[a] The numbers in parentheses are taken from crystallographic data as given by ref 32.

gallophosphate and 1.90 Å in the Zn-, Mn-, and Mg-substituted materials. From a short literature survey[11−13,23−29,32,34] it is concluded that 4-fold, tetrahedral coordination of Ga atoms in gallophosphate materials leads to average bond distances of 1.82 Å, 5-fold, trigonal-bipyramidal coordination gives $d_{Ga-O,av}$ of ∼1.89 Å and average bond distances of ∼1.96 Å are found for 6-fold, octahedral coordination states of Ga.

The EXAFS spectra of the Co, Zn, and Mn K-edges together with the corresponding FTs and best fits are shown in Figure 8. On the basis of the crystal structure of $NH_4[CoGa_2P_3O_{12}(H_2O)_2]$[32] the data were fit with a model containing three O shells and two P shells. As can be seen in Figure 1, Co is surrounded by three pairs

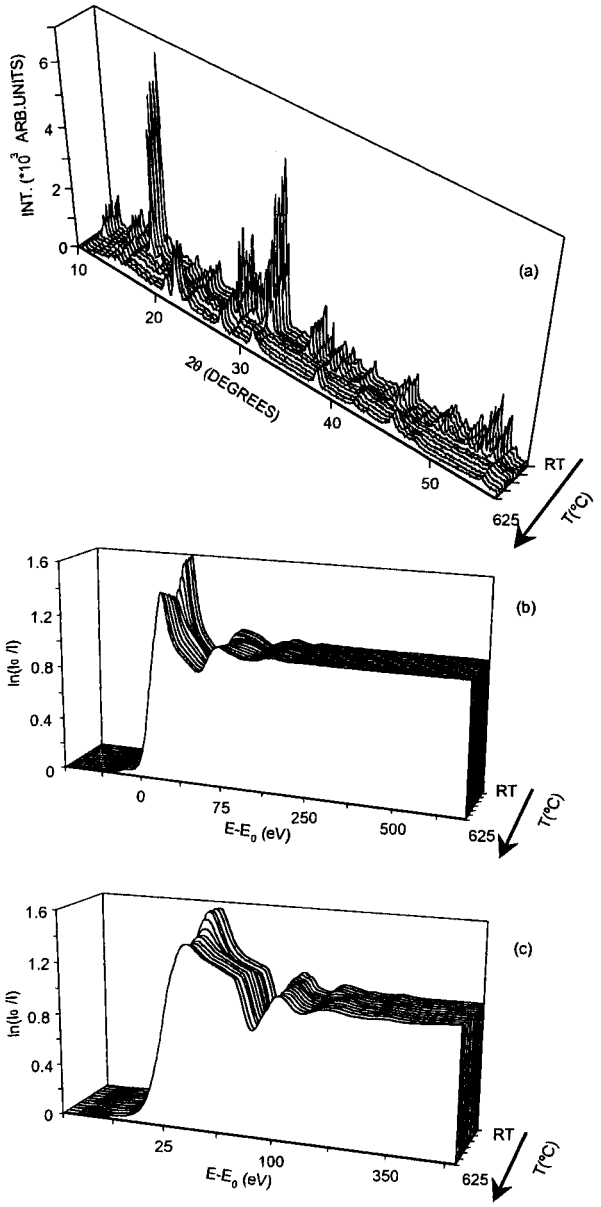

Figure 9. Combined EXAFS/XRD following the decomposition of $NH_4[CoGa_2P_3O_{12}(H_2O)_2]$ and the appearance of a new crystalline phase: (a) X-ray diffraction pattern, (b) Co K-edge EXAFS, and (c) Ga K-edge EXAFS.

of equivalent O atoms as its nearest neighbors and three P atoms distributed over two crystallographically different positions as its next nearest neighbors. Identical to the refinement of the Ga K-edges multiple scattering was implemented in the calculation. The structural parameters of the EXAFS data analysis are given in Table 5. The bond distances and bond angles obtained in this manner for $NH_4[CoGa_2P_3O_{12}(H_2O)_2]$ are in reasonable agreement with the crystallographic data. Furthermore, it can be seen that the Mn−O distances are longer than the Co−O and Zn−O distances found for $NH_4[CoGa_2P_3O_{12}(H_2O)_2]$ and $NH_4[ZnGa_2P_3O_{12}(H_2O)_2]$. This is in line with the larger ionic radius of the Mn ion as compared to Co and Zn.

Apart from the investigation of the structural chemistry by the suite of techniques as described above, we were interested in the thermal stability of these materials, i.e. retention of the microporous structure at elevated temperatures. This can be evaluated by using

the combined EXAFS/XRD method. This technique has the great advantage of probing, under identical conditions, both short-range and long-range order. This methodology has been successfully used by some of us[43,44] in predicting the catalytic nature of the microporous solids in many metal-substituted ALPO systems. We have applied this method to all the materials studied here, in particular probing the heterometal ion and Ga by recording the K-edge X-ray absorption spectra during the course of the heat treatment process (removal of template). The main common feature that is derived from this investigation is that the materials lose their microporous structure upon removal of the ammonium template molecule and the coordinating water molecules.

A typical measurement is shown in Figure 9. From these experiments it follows that all metal-substituted gallophosphates described here become amorphous at elevated temperatures, with $NH_4[CoGa_2P_3O_{12}(H_2O)_2]$ being the most stable collapsing at ~400 °C and the iron-containing material, $NH_4[FeGa_2P_3O_{12}(H_2O)_2]$, being the least stable with a decomposition temperature of about 220 °C. At temperatures close to 600 °C a new crystalline phase becomes apparent in the XRD pattern which has not been further identified.

It appears that catalytic applications of gallophosphates and/or metal-substituted gallophosphates are hampered by the thermal instability of these materials. In contrast to the aluminophosphate molecular sieves it is difficult to remove the template or solvent molecules from the channels of these materials without collapse of their porous structure. The presence of tiny amounts of water might play a crucial role in this process but further investigations have to be carried out in this direction in order to exploit the microporous nature of these materials because just as their aluminum counterparts gallophosphates possess a large structural flexibility and can incorporate heteroatoms as has been shown here.

Acknowledgment. The authors thank EPSCRC for financial support and CLRC for providing access to SRS facilities. The authors also thank Dr. A. M. van der Kraan for measurement of the Mössbauer data, G. H. Nachtegaal of the NSR center, Nijmegen, The Netherlands, for her assistance in measuring the ^{71}Ga MAS NMR spectra, and A. M. Elemans-Mehring for her assistance in the chemical analysis.

CM9806331

(43) Thomas, J. M.; Greaves, G. N.; Sankar, G.; Wright, P. A.; Chen, J.; Dent, A. J.; Marchese, L. *Angew. Chem., Int. Ed. Engl.* **1994**, *33*, 1871.

(44) Barrett, P. A.; Sankar, G.; Catlow, C. R. A.; Thomas, J. M. *J. Phys. Chem. Solids* **1995**, *56*, 1395.